Enlargement of zero averaged refractive index gaps in the photonic heterostructures containing negative-index materials

Yuanjiang Xiang, Xiaoyu Dai, Shuangchun Wen,* and Dianyuan Fan
Research Center of Laser Science and Engineering and School of Computers and Communication, Hunan University, Changsha 410082, China

(Received 23 May 2007; published 9 November 2007)

We show that the frequency range of the zero averaged refractive index gap in a photonic heterostructure containing negative-index materials can be enlarged owing to the property that its lower and upper frequency edges depend on the thickness ratio of the positive- and negative-index materials. Compared to the zero averaged refractive index gap of a single photonic crystal, the frequency range of the zero averaged refractive index gaps in a photonic heterostructure can be notably enlarged. Moreover, it is shown that the band edge of the zero averaged refractive index gap is determined not only by the TM polarization but also by the TE polarization, which is obviously different from the omnidirectional band gaps in conventional photonic crystals, whose bandwidth is determined by the TM polarization.

DOI: 10.1103/PhysRevE.76.056604 PACS number(s): 41.20.Jb, 42.70.Qs, 78.20.Ci

I. INTRODUCTION

Photonic crystals (PCs) made of periodic dielectric materials in one, two, or three spatial directions that exhibit stop bands or photonic band gaps (PBGs) have been investigated intensively because of their ability to control the propagation of light and the possibility of many new optical devices [1,2]. It has been proved that the Bragg scattering in a periodic dielectric structure is the reason for the formation of a PBG. If the PBG can reflect electromagnetic waves incident at any angle with any polarization, then an omnidirectional band gap (OBG) can be achieved with negligible loss within a specific frequency range in a one-dimensional photonic crystal (1DPC) [3–6]. Such an OBG has potential applications in improving planar microcavities [7], optical fibers [8], Fabry-Pérot resonators [9], etc. The width of the OBG plays an important role in the applications of 1DPC omnidirectional reflectors. It has been demonstrated by some authors [10–13] that the frequency range of OBGs can be enlarged by a photonic heterostructure, made by combining two or more 1DPCs.

On the other hand, some researchers have attempted to realize an OBG in negative-index materials (NIMs). NIMs with simultaneously negative permittivity and negative permeability, which were first suggested theoretically by Veselago [14], have received a great deal of attention due to the experimental realization of such materials at optical frequencies [15] and the theoretical awareness of using a NIM slab as a perfect lens [16]. 1DPCs composed of alternating layers of positive-index materials (PIMs) and NIMs have already been investigated through calculating the transmittance or the reflectance of the structures [17], and it has been shown that these PCs possess zero-average-index (zero-$\bar{n}$) gaps. As the incidence angle increases, the frequency shift of the band edge of the zero-$\bar{n}$ gap is small for both polarizations [18]; hence the zero-$\bar{n}$ gap can also be used as an omnidirectional total reflector. However, the width of the OBG for this 1DPC is very narrow, making these structures inefficient in application as omnidirectional total reflectors. Nevertheless, Bloemer *et al.* have proposed one way to enlarge the omnidirectional reflection band for a single layer of a NIM [19], but this way is not applicable in a multilayered PC.

In this paper, based on the systematic investigation of the properties of OBGs in 1DPCs containing NIMs, we present a method to enlarge the frequency range of OBGs by changing the thickness ratio of the different materials in the photonic heterostructures, which to our knowledge seems not to have been considered in previous research. Our study has been carried out in two steps. First, we investigate systemically the properties of OBGs in 1DPCs containing NIMs in Sec. II, giving the mathematical formulation based on the transfer matrix method [18,20], and its application to the case of a 1DPC consisting of NIMs. The omnidirectional total reflection frequency range of this structure was then determined. Second, we demonstrated the method for enlargement of the frequency range of omnidirectional total reflection in Sec. III; an enlargement in the omnidirectional total reflection frequency range was observed in this heterostructure as com-

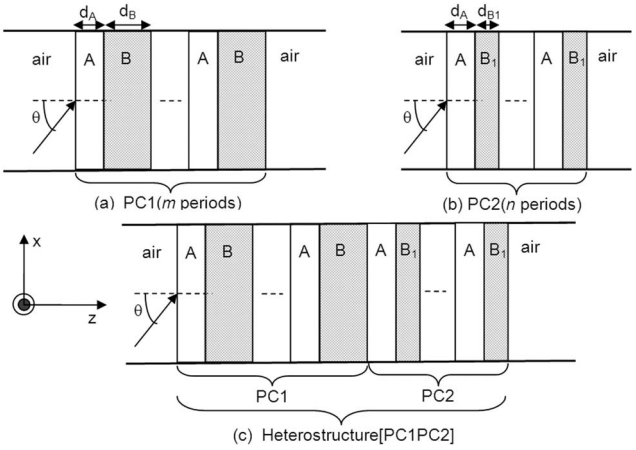

FIG. 1. Structures of photonic crystals for (a) PC1, (b) PC2, and (c) heterostructure PC1/PC2.

*Corresponding author. scwen@vip.sina.com

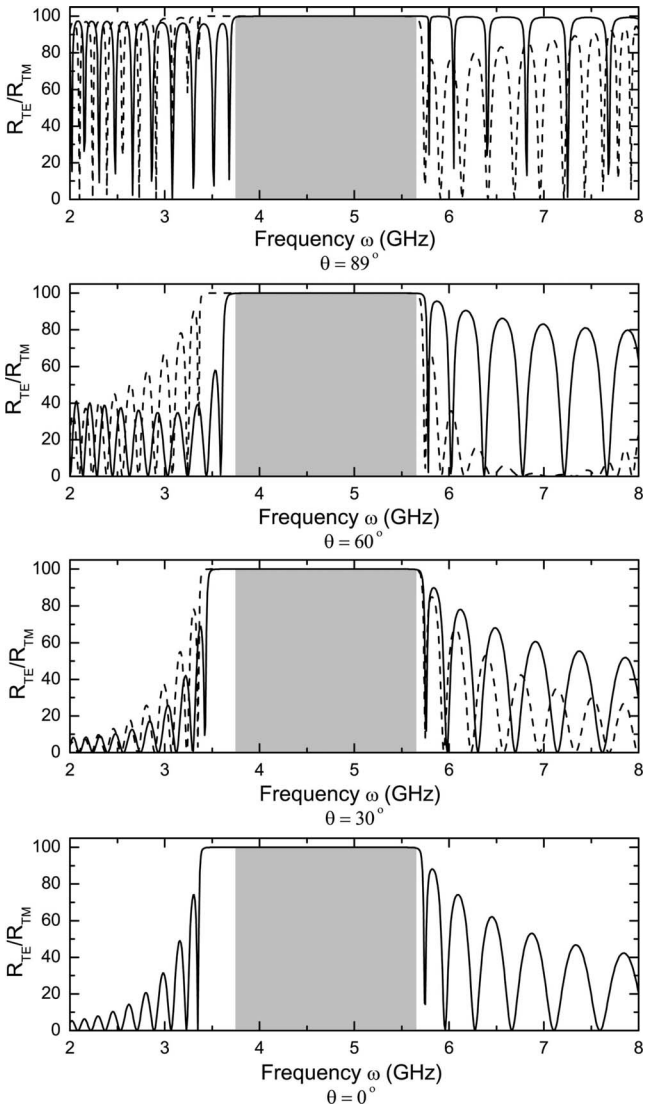

FIG. 2. Reflectivity spectra of PC1 at various incident angles. The solid (dashed) lines are for TE (TM) polarization. The gray area is the total omnidirectional band gap.

pared to the single PC. The results obtained are summarized in Sec. IV.

II. OMNIDIRECTIONAL ZERO-$\bar{n}$ GAP AND TRANSFER MATRIX METHOD

1DPCs composed of alternating layers of NIMs and PIMs are shown in Fig. 1. PC1 $[(AB)^m]$ and PC2 $[(AB_1)^n]$ are two different 1DPCs. A and B (B_1) indicate NIMs and PIMs, respectively, and m (n) is the period number. Here we suppose that the relative permittivity and permeability in the NIMs are given by

$$\varepsilon_A = a - \omega_{ep}^2/\omega^2, \quad \mu_A = b - \omega_{mp}^2/\omega^2, \tag{1}$$

where a and b are positive constants, and ω_{ep} and ω_{em} are the electronic plasma frequency and magnetic plasma frequency, respectively. In the frequency range of $\omega^2 < (\omega_{ep}^2/a, \omega_{mp}^2/b)$, ε_A and μ_A are negative simultaneously. In the following calculation, we choose $a=1.21$, $b=1$, and $\omega_{ep}=\omega_{em}=10$ GHz. Similar forms to ε_A and μ_A chosen in the present paper have been used theoretically [18,21,22] and experimentally [23,24] in previous reports. The thicknesses of NIM and PIM in two 1DPCs are assumed to be d_A and d_B, respectively. Here, we assume $d_A=12$ mm, $d_B=24$ mm, $\varepsilon_B=1$, $\mu_B=1$, and $m=n=20$. Under these conditions, when $n_{Az}d_A+n_{Bz}d_B=0$, the effective zero-refractive-index condition $[\bar{n}=(1/d)\int_0^d n(z)dz=0]$ will be satisfied; then the zero-$\bar{n}$ band gap will occur where $n_{Az}=-\sqrt{\varepsilon_A\mu_A-\sin^2\theta}$ and $n_{Bz}=\sqrt{\varepsilon_B\mu_B-\sin^2\theta}$. $d=d_A+d_B$ is the period of the unit cell and θ is the incident angle.

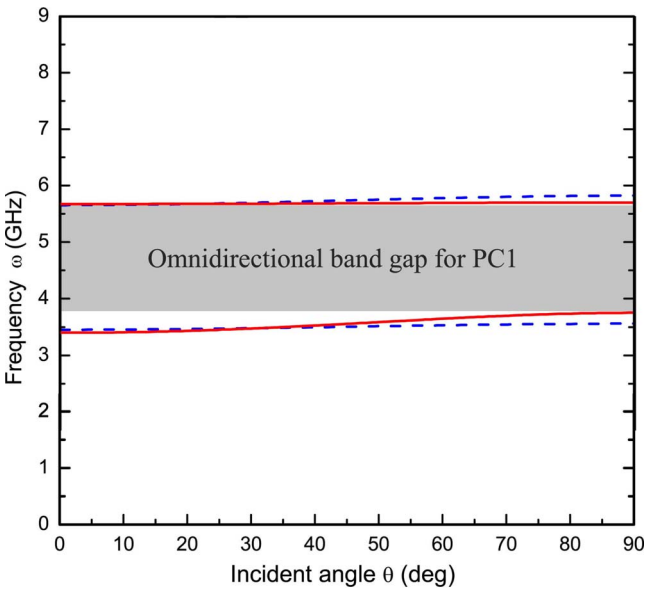

FIG. 3. (Color online) Photonic band structure of PC1 in terms of angular frequency and incident angle. The solid (dashed) lines are for TE (TM) polarization bands. The gray area is the total omnidirectional band gap.

We use the transfer-matrix method (TMM) [18,20] to analyze the OBGs of the structure. Let a plane wave be injected from vacuum at an angle θ into the 1DPC with $+z$ direction. Generally, the electric (E_y) and magnetic (H_x) fields at any two positions z and $z+\Delta z$ (for the PIM or NIM layer) within the same layer can be related via a transfer matrix,

$$M_j(\Delta z,\omega) = \begin{pmatrix} \cos(k_z^j\Delta z) & -i\dfrac{1}{p_j}\sin(k_z^j\Delta z) \\ -ip_j\sin(k_z^j\Delta z) & \cos(k_z^j\Delta z) \end{pmatrix}, \tag{2}$$

where $k_z^j=(\omega/c)\sqrt{\varepsilon_j}\sqrt{\mu_j}\sqrt{1-\sin^2\theta/(\varepsilon_j\mu_j)}$ is the component of the wave vector along the z axis in the medium A or B, $p_j=(\sqrt{\varepsilon_j}/\sqrt{\mu_j})\sqrt{1-\sin^2\theta/(\varepsilon_j\mu_j)}$ for the TE polarization and $p_j=(\sqrt{\mu_j}/\sqrt{\varepsilon_j})\sqrt{1-\sin^2\theta/(\varepsilon_j\mu_j)}$ for the TM polarization, and $j=A,B$ denote the NIM and PIM layers, respectively.

The transmission coefficient of the monochromatic plane wave can be obtained from the TMM [18,20]

$$t(\omega) = \frac{2q_0}{(q_s x_{11}+q_0 x_{22})q_0+(q_0 q_s x_{12}+x_{21})}, \tag{3}$$

where $q_0=q_s=(\sqrt{\varepsilon_0}/\sqrt{\mu_0})\sqrt{1-\sin^2\theta/(\varepsilon_0\mu_0)}=\cos\theta$ for the vacuum $(\varepsilon_0=\mu_0=1)$ of the space $z<0$ before the incidence

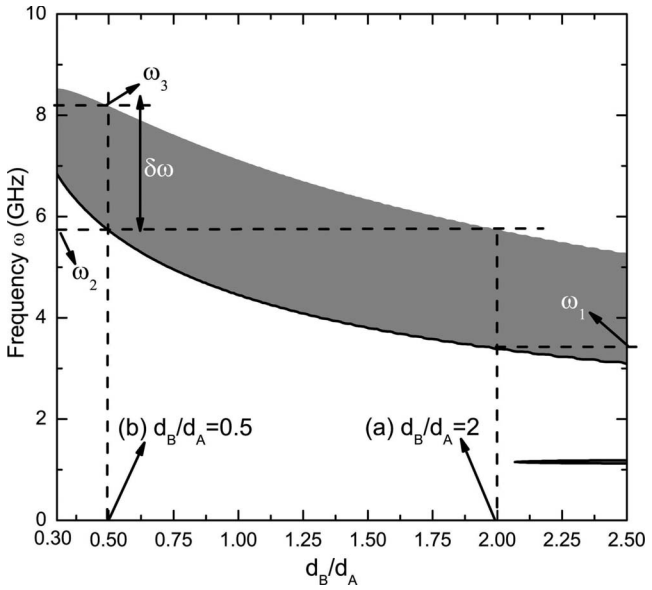

FIG. 4. Photonic band structure of photonic crystal in terms of angular frequency and thickness ratio of media B and A at normal incidence. The gray area is the frequency range of this band gap. The frequency range for two different thickness ratios are shown in the figure, for d_B/d_A=(a) 2 and (b) 0.5.

end and the space $z>L$ after the exit end, where L is the total length of the 1DPC. x_{ij} $(i,j=1,2)$ are the matrix elements of $X_N(\omega)=\Pi_{j=1}^{2N}M_j(d_j,\omega)$, which represents the total transfer matrix connecting the fields at the incidence and exit ends.

For an infinite periodic structure $(N\to\infty)$, according to Bloch's theorem, the dispersion at any incident angle follows the relation [17,25]

$$\cos(q_z d) = \cos(k_z^A d_A)\cos(k_z^B d_B) - \frac{1}{2}\left(\frac{p_B}{p_A}+\frac{p_A}{p_B}\right)\sin(k_z^A d_A)\sin(k_z^B d_B), \quad (4)$$

where q_z is the z component of the Bloch wave vector. When the absolute value of the right-hand side of Eq. (4) is larger than 1, Eq. (4) has no real solution for q_z, which corresponds to the band gap of the PC. We will adopt this dispersion equation to calculate the zero-$\bar{n}$ band gaps.

First, we discuss the optical transmission spectra of PC1. Figure 2 gives the dependence of the PBGs on the incident angle. The gray area is the total OBG. It is demonstrated that the zero-$\bar{n}$ gap is insensitive to the incident angle for TM polarization but sensitive for TE polarization. The frequency shift of the edges of the zero-$\bar{n}$ gap is small when the incident angle increases for TM polarization. But such a frequency shift should not be ignored when it is used as a omnidirectional total reflector. It can be seen that the upper band edge is insensitive to the increase of the incident angle for both polarizations, and the frequency shift of the lower band edge for the TE modes upward to high frequency as the incident angle increases, but the case for TM modes is contrary, with a frequency shift downward to low frequency. It can also be seen from Fig. 2 that there is an OBG for TE polarization in the displayed frequency range, from 3.8 to 5.7

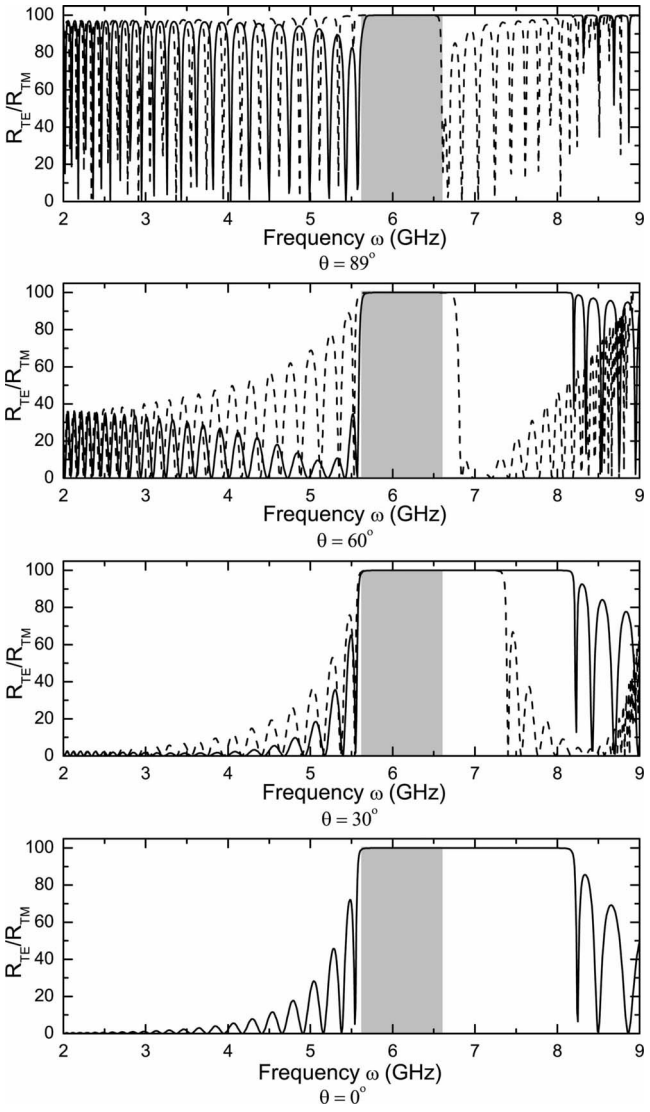

FIG. 5. Reflectivity spectra of PC2 at various incidence angles. The solid (dashed) lines are for TE (TM) polarization. The gray area is the total omnidirectional band gap.

GHz. For the TM polarization, the OBG spans from 3.3 to 5.6 GHz. We thus can obtain the overall frequency range of the OBG for any polarization from 3.8 to 5.6 GHz, and the frequency bandwidth is $\Delta\omega$=1.8 GHz, which is determined by the frequency range at the grazing incidence $(\theta\sim 90°)$ of both polarizations, viz., the OBGs in this 1DPC exist between the upper frequency edge at $\theta\sim 90°$ for TM polarization and the lower frequency edge at $\theta\sim 90°$ for TE polarization. This property is different obviously from that of omnidirectional total reflection in a conventional 1DPC [3,4], in which the TM band gap determines the bandwidth of the omnidirectional total reflector, since the TM PBG is narrower than the TE one, except for normal incidence.

For comparison, we plot the dependence of the PBGs on the incident angle and angular frequency for TE and TM polarizations in Fig. 3, where the white areas correspond to propagation bands and the black areas denote the forbidden bands representing reflectance (R) approaching 1 $(R\sim 1)$. The gray region is the omnidirectional PBG. The gap lies in

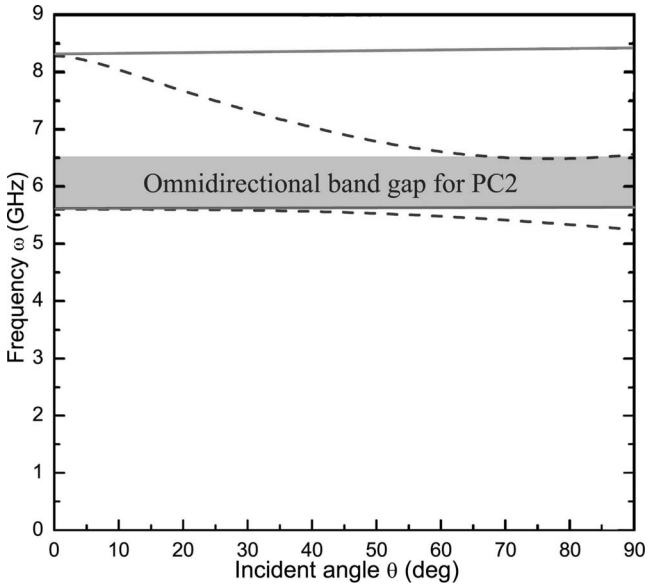

FIG. 6. Photonic band structure of PC2 in terms of angular frequency and incident angle. The solid (dashed) lines are for TE (TM) polarization bands. The gray area is the total omnidirectional band gap.

the frequency range 0–9 GHz, which is the zero-$\bar{n}$ band gap. From Fig. 3, we can also see that the OBG frequency region runs from 3.8 to 5.6 GHz and the frequency width $\Delta\omega$ is 1.8 GHz. These results are identical to those in Fig. 2.

III. ENLARGEMENT OF THE ZERO-$\bar{n}$ GAP FREQUENCY RANGE

We now discuss how to enlarge the zero-$\bar{n}$ gap frequency ranges. In Fig. 4, we show the dependence of the gap on the thickness ratio of the two media at normal incidence angle for TE polarization for lattice constant $d=12$ mm. It can be seen from Fig. 4 that the frequency range of zero-$\bar{n}$ gap can be modified by changing the thickness ratio. Such properties of the zero-$\bar{n}$ gap are useful for designing periodic structures with wider ODGs. It can also be seen that the width of this gap changes little when the ratio $d_B/d_A>1$; however, if $d_B/d_A<0.5$, the width of this gap obviously becomes narrower. Moreover, the lower and upper edges of the zero-$\bar{n}$ gap are affected by the thickness ratio, i.e., the lower and upper edges of the zero-$\bar{n}$ gap shift to lower frequency as the thickness ratio of the two media increases. Hence, the zero-$\bar{n}$ gap can be widened by using photonic heterostructures which are constructed from two or more PCs having different thickness ratios d_B/d_A.

In order to achieve the optimal width of the ODGs, we present the criteria for designing the broadband reflector as follows. First, we can get the frequency range of the lower and upper band gap edges for PC1 according to the thickness ratio $d_B/d_A=2$, which are ω_1 and ω_2, respectively. Then we plot a line for the upper band gap edges ω_2 from right to left, and we can get the point of intersection between this line and the lower band gap edge; according to this point, we can derive the optimal thickness ratio, which corresponds to

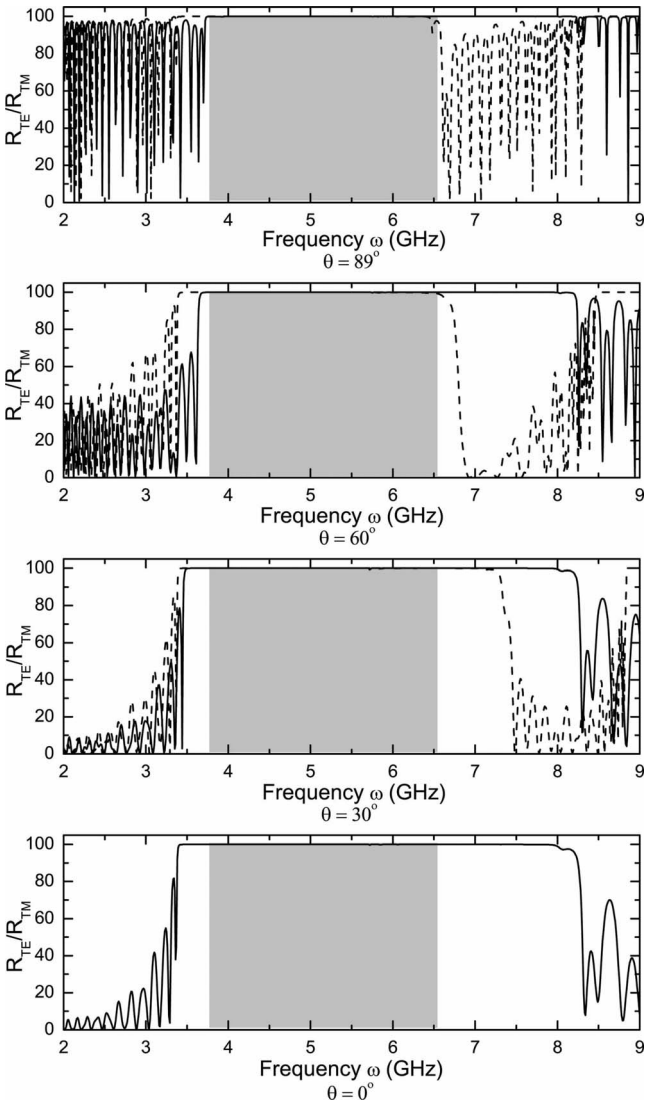

FIG. 7. Reflectivity spectra of heterostructure PC1/PC2 at various incidence angles. The solid (dashed) lines are for TE (TM) polarization. The gray area is the total omnidirectional band gap.

$d_B/d_A=0.5$. We then can design a photonic crystal (PC2) satisfying this condition, as shown in Fig. 1(b), where $d_B=6$ mm and other parameters are not changed. Hence we need not change the physics parameters of media A and B, and only need to change the thickness of the medium B to get a wider-band-gap omnidirectional total reflector. Moreover, the recent experimental results show that these 1DPCs can be fabricated by using a composite right- and left-handed transmission line [23,24]. It is easy to design practical optical components with wider omnirectional zero-$\bar{n}$ gap. For other thickness ratios of PC1, we can adopt a similar method to get the thickness ratio of PC2. This method assures that the OBGs of two sub-PCs are adjacent to each other and the width of the OBG of the heterostructure is optimal.

The reflectivity spectra of PC2 for the TE and TM polarizations for different incidence angles are shown in Fig. 5, where $d_A=12$ mm and $d_B=6$ mm. We can see that, when the thickness ratio is small, the band gap of TM polarization is very sensitive to increase of the incident angle, which is

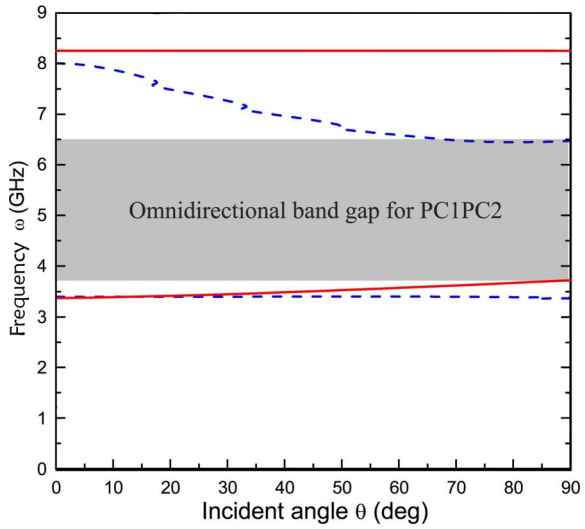

FIG. 8. (Color online) Photonic band structure of heterostructure PC1/PC2 in terms of angular frequency and incidence angle. The solid (dashed) lines are for TE (TM) polarization bands. The gray area is the total omnidirectional band gap.

different from the case when the thickness ratio is large. Moreover, the lower band gap edge of this PC2 is insensitive to a change of the incidence angle of the TE polarization, which is in contrast to the OBG of PC1. Figure 6 shows the band structure of PC2. From Figs. 5 and 6, it can be seen that the OBG for TE polarization is from 5.6 to 8.25 GHz and the OBG for TM polarization is from 5.5 to 6.6 GHz. The overall OBG for any polarization is determined by the frequency range at the grazing incidence of both polarizations, from 5.6 to 6.6 GHz. Hence the bandwidth of PC2 is 1.0 GHz. It is worth noting that the frequency range of the OBG for PC2 is much narrower than the OBG for PC1 because the thickness ratio of the layers is reversed. In general, for $d_B/d_A<1$, the widths of the OBGs are smaller than those for $d_B/d_A>1$. Comparing Figs. 5 and 6 with Figs. 2 and 3, we find that we can combine the two PCs (PC1 and PC2) to form a heterostructure because the OBG of PC2 is adjacent to the OBG of PC1.

The devised heterostructure is shown in Fig. 1(c), and the reflectivity spectra and band structure are shown in Figs. 7 and 8, respectively. From these figures, we can see that a wider-bandwidth OBG has been obtained. There exists an OBG for TE polarization in the frequency range from 3.8 to 8.25 GHz, and for TM polarization it spans from 3.4 to 6.6 GHz. The overall OBG is from 3.8 to 6.6 GHz and the bandwidth for this heterostructure is $\Delta\omega=2.8$ GHz. Here an increase of 1.0 and 1.8 GHz in the bandwidth of the OBG as compared to PC1 and PC2, respectively, was observed. From the aforementioned discussions, the total OBG frequency range is substantially enlarged for all incidence angles and for both TM and TE polarizations. Consequently, the omnidirectional total reflection frequency range for any polarization is enlarged. It is obvious that, by the method developed in this paper, one can use more 1DPCs to form multiple photonic heterostructures to get a very wide omnidirectional zero-$\bar{n}$ band gap frequency range under the condition that the directional PBGs of the adjacent 1DPCs at any incidence angle overlap each other in tandem. The wider-bandwidth zero-$\bar{n}$ gaps have potential applications in microcavities, antenna substrates, and coaxial waveguides, etc.

It should be pointed out that the loss of NIMs cannot be neglected, though the imaginary parts of the permittivity and permeability at some frequencies are very low. The main properties of the omnidirectional zero-$\bar{n}$ gap, however, are not affected because the PBG [determined by Eq. (4)] does not present any rapid change when a very small loss is added to the material. The loss affects only the magnitude of transmission.

IV. CONCLUSION

A method to enlarge the zero-$\bar{n}$ gap frequency range by using a photonic heterostructure containing NIMs has been proposed and demonstrated. We can first get a new sub-PC by changing the thickness ratio of the PIM and NIM, and then obtain a photonic heterostructure through the combination of the new sub-PC with a PC designed in advance. We have shown that a wide-band omnidirectional zero-$\bar{n}$ gap can be obtained in such a photonic heterostructure. The idea of using photonic multiple heterostructures designed by our method may provide a simple and effective way to solve the problem of enlarging the frequency range of the zero-$\bar{n}$ gap, suggesting potential applications in improving planar microcavities, optical fibers, and Fabry-Pérot resonators, etc. Moreover, it is shown that the zero-$\bar{n}$ gap is sensitive to the incidence angle when the thickness ratio is small, and the band edges of the high- and low-frequency limits are determined by TM polarization and TE polarization, respectively, at larger incidence angles.

ACKNOWLEDGMENTS

This work is supported by the National Natural Science Foundation of China (Grants No. 10674045 and No. 10576012), the Program for New Century Excellent Talents in University, and the Specialized Research Fund for the Doctoral Program of Higher Education of China (Grant No. 20040532005).

[1] E. Yablonovitch, Phys. Rev. Lett. **58**, 2059 (1987).
[2] S. John, Phys. Rev. Lett. **58**, 2486 (1987).
[3] N. Winn, Y. Fink, S. Fan, and J. D. Joannopoulos, Opt. Lett. **23**, 1573 (1998).
[4] Y. Fink, J. N. Winn, S. Fan, C. Chen, J. Michel, J. D. Joannopoulos, and E. L. Thomas, Science **282**, 1679 (1998).
[5] D. N. Chigrin, A. V. Lavrinenko, D. A. Yarotsky, and S. V. Gaponenko, Appl. Phys. A: Mater. Sci. Process. **68**, 25 (1999).

[6] A. Mir, A. Akjouj, E. H. El Boudouti, B. Djafari-Ronhani, and L. Dobrzynski, Vacuum **63**, 197 (2001).
[7] J. A. E. Wasey and W. L. Barnes, J. Mod. Opt. **47**, 725 (2000).
[8] M. Ibanescu, Y. Fink, S. Fan, E. L. Thomas, and J. D. Joannopoulos, Science **289**, 415 (2000).
[9] I. Abdulhalim, Opt. Commun. **215**, 225 (2003).
[10] A. Sharkawy, S. Shi, and D. W. Prather, Appl. Opt. **41**, 7245 (2002).
[11] E. L. Ivchenko, M. M. Voronov, M. V. Erementchouk, L. I. Deych, and A. A. Lisyansky, Phys. Rev. B **70**, 195106 (2004).
[12] X. Wang, X. H. Hu, Y. Z. Li, W. L. Jia, C. Xu, X. H. Liu, and J. Zi, Appl. Phys. Lett. **80**, 4291 (2002).
[13] W. H. Southwell, Appl. Opt. **38**, 5464 (1999).
[14] V. G. Veselago, Sov. Phys. Usp. **10**, 509 (1968).
[15] V. M. Shalaev, Nat. Photonics **1**, 41 (2007).
[16] J. B. Pendry, Phys. Rev. Lett. **85**, 3966 (2000).
[17] J. S. Li, L. Zhou, C. T. Chan, and P. Sheng, Phys. Rev. Lett. **90**, 083901 (2003).
[18] H. T. Jiang, H. Chen, H. Q. Li, Y. W. Zhang, and S. Y. Zhu, Appl. Phys. Lett. **83**, 5386 (2003).
[19] M. Bloemer, G. D'Aguanno, M. Scalora, and N. Mattiucci, Appl. Phys. Lett. **87**, 261921 (2005).
[20] M. Born and E. Wolf, *Principles of Optics*, 7th (expanded) ed. (Cambridge University Press, Cambridge, U.K., 1999).
[21] D. R. Smith and N. Kroll, Phys. Rev. Lett. **85**, 2933 (2000).
[22] R. W. Ziolkowski, Phys. Rev. E **70**, 046608 (2004).
[23] G. V. Eleftheriades, A. K. Iyer, and P. C. Kremer, IEEE Trans. Microw. Theory Tech. **50**, 2702 (2002).
[24] L. W. Zhang, Y. W. Zhang, L. He, H. Q. Li, and H. Chen, Phys. Rev. E **74**, 056615 (2006).
[25] L. G. Wang, H. Chen, and S. Y. Zhu, Phys. Rev. B **70**, 245102 (2004).